

Intermediate expression of CCRL1 reveals novel subpopulations of medullary thymic epithelial cells that emerge in the postnatal thymus

Ana R. Ribeiro^{1,2}, Catarina Meireles^{1,2}, Pedro M. Rodrigues^{1,2} and Nuno L. Alves¹

¹ Thymus Development and Function Laboratory, Institute for Molecular and Cellular Biology, Porto, Portugal

² Institute for Biomedical Sciences Abel Salazar, University of Porto, Porto, Portugal

Originally published in European Journal of Immunology. 2014 Oct;44(10):2918-24. Epub september, 5, 2014.

Doi: 10.1002/eji.20144458

Cortical and medullary thymic epithelial cells (cTECs and mTECs, respectively) provide inductive microenvironments for T-cell development and selection. The differentiation pathway of cTEC/mTEC lineages downstream of common bipotent progenitors at discrete stages of development remains unresolved. Using IL-7/CCRL1 dual reporter mice that identify specialized TEC subsets, we show that the stepwise acquisition of chemokine (C-C motif) receptor-like 1 (CCRL1) is a late determinant of cTEC differentiation. Although cTECs expressing high CCRL1 levels (CCRL1^{hi}) develop normally in immunocompetent and *Rag2*^{-/-} thymi, their differentiation is partially blocked in *Rag2*^{-/-}*Il2rg*^{-/-} counterparts. These results unravel a novel checkpoint in cTEC maturation that is regulated by the cross-talk between TECs and immature thymocytes. Additionally, we identify new *Ulex europaeus* agglutinin 1 (UEA)⁺ mTEC subtypes expressing intermediate CCRL1 levels (CCRL1^{int}) that conspicuously emerge in the postnatal thymus and differentially express *Tnfrsf11a*, *Ccl21*, and *Aire*. While rare in fetal and in *Rag2*^{-/-} thymi, CCRL1^{int} mTECs are restored in *Rag2*^{-/-} Marilyn TCR-Tg mice, indicating that the appearance of postnatal-restricted mTECs is closely linked with T-cell selection. Our findings suggest that alternative temporally restricted routes of new mTEC differentiation contribute to the establishment of the medullary niche in the postnatal thymus.

INTRODUCTION

Within the thymus, it is well established the role of distinct thymic epithelial cell (TEC) microenvironments in supporting the generation of functionally diverse and self-tolerant T cells 1. While cortical TECs (cTECs) promote T-cell lineage commitment and positive selection, medullary TECs (mTECs) participate in the elimination of autoreactive T cells and the differentiation of Treg cells 2. In particular, auto-immune regulator (Aire)⁺ mTECs have an established role in tolerance induction 3. Cortical and medullary TECs are derived from common bipotent progenitors present within the fetal and postnatal thymus 4, 5. Importantly, the cTEC/mTEC maturation pathways downstream of bipotent progenitors, as well as the requirements for the establishment of these specialized compartments at discrete stages of development are still unresolved.

The cTEC/mTEC lineage specification branches early in embryonic development 6. During initial stages of gestation, the thymic epithelium predominately comprises Ly51⁺CD205⁺β5t⁺ cTECs 7-9, and mature mTECs, including Aire⁺ mTECs, first appear around embryonic day 16 (E16) 10, 11. The emergence of embryonic mTECs depends on cellular interactions with lymphoid tissue inducer cells and invariant γδ T cells 12, 13, and involves signaling through TNFR superfamily receptor activator of NF-κB (RANK) and lymphotoxin beta receptor (LTβR) expressed on TEC precursors 12, 14. However, and despite the elucidation of distinct maturation stages in mTECs 2, there are still gaps in the understanding of cTEC differentiation. We, and others, have recently

demonstrated that fetal TEC progenitors expressing cortical properties are able to generate mTECs 15-17. These reports support the idea that embryonic TEC precursors progress transitionally through the cortical lineage prior to commitment to the medullary pathway, emphasising that TEC differentiation is more complex than previously recognized 18.

The size of the medullary epithelial microenvironment continues to expand after birth, fostered by additional interactions between TECs and mature thymocytes, namely positively selected and CD4 single positive (SP4) thymocytes 2. The concerted activation of RANK-, LT β R-, and CD40-mediated signaling on mTECs and their precursors completes the formation of the adult medullary niche 2. It has been previously demonstrated a clonal nature for discrete embryonic mTEC islets, which progressively coalesce into larger medullary areas in the adult thymus 10, 19. Hence, one can argue that the adult mTEC niche exclusively results from the expansion of embryonic-derived mTECs and their precursors. Still, it remains possible that alternative developmental stage-specific pathways participate in the organization of the adult mTEC niche.

Here, we report a novel checkpoint in cTEC differentiation, which is defined by the sequential acquisition of chemokine (C-C motif) receptor-like 1 (CCRL1) expression and is compromised in mice with profound blocks in early T-cell development. Additionally, we define original subsets of mTECs, characterized by the intermediate CCRL1 expression, that emerge in the postnatal thymus in tight association with thymocytes that develop beyond the TCR β selection. Our findings provide evidence for the existence of several waves of mTEC development in the embryonic and postnatal thymus.

RESULTS AND DISCUSSION

Acquisition of CCRL1 expression is a late cTEC determinant

The expression of CCRL1, an atypical chemokine receptor that controls the bioavailability of key chemoattractants CCL19, CCL21, and CCL25, identifies cTECs in the postnatal thymus 20. Given the incomplete knowledge on the differentiation of CCRL1⁺cTECs, we assessed their generation using previously generated IL7^{YFP}-CCRL1^{GFP} dual reporter mice 15. While in IL7^{YFP}reporter mice, YFP expression is a surrogate of a subtype of cTECs expressing abundant levels of the crucial thymopoietin IL-7 (IL7^{YFP+}) 8, 15, in CCRL1^{GFP} reporter mice, GFP expression labels cTECs in the postnatal thymus 20. We previously showed that postnatal IL7^{YFP+} TECs locate within cTECs that express high CCRL1 levels (referred as CCRL1^{hi}) 15. Here, analysis during early stages of thymic development showed that the emergence of IL7^{YFP+}, CD205⁺, and Ly51⁺ TECs around E12.5–13.5 preceded the appearance of CCRL1-expressing cells (Fig. 1A and Supporting information Fig. 1B; nonreporter thymi in Supporting Information Fig. 1A). During the E12.5–15.5 period, both IL7^{YFP+} and remaining YFP⁻ cTECs progressively acquired the expression of CCRL1. At E18.5, and similarly to the postnatal thymus 15, IL7^{YFP+} TECs reside within CCRL1^{hi} cells (Fig. 1A). The number of CCRL1^{hi}cTECs gradually increased throughout development, contributing to the expansion of TEC cellularity during perinatal life. TECs lacking CCRL1 and expressing intermediate CCRL1 levels (referred as CCRL1⁻ and CCRL1^{int}, respectively) followed steadier numbers during this period (Fig. 1B). To address whether the acquisition of CCRL1 defined a late cTEC maturation stage dependent on signals provided by developing thymocytes, we crossed double reporter mice onto a *Rag2*^{-/-} or *Rag*^{-/-}*Il2r*^{-/-} background. While the majority of TECs were CCRL1^{hi} in the postnatal *Rag*^{-/-} thymus, we detected an accumulation of CCRL1^{int} TECs in the *Rag2*^{-/-}*Il2rg*^{-/-} thymus (Fig. 1C and D, nonreporter thymi in Supporting Information Fig. 1C), akin to the CCRL1 pattern observed at E15.5 (Fig. 1A). Contrarily to CCRL1, the expression of Ly51, CD205, *Psm11* (β 5t), and *Ctsl* was not impaired in TECs from *Rag2*^{-/-}*Il2rg*^{-/-} thymi (Supporting Information Fig. 1D and E) 8, 15. CCRL1⁻ and CCRL1^{int} TECs in the *Rag2*^{-/-}*Il2rg*^{-/-} thymus were distinct from immunocompetent counterparts, as in the later these subsets comprised mostly mTECs (below in Fig. 2) that are virtually absent in the *Rag2*^{-/-}*Il2rg*^{-/-} thymus 8. The partial blockade in CCRL1, CD40, and MHCII expression in *Rag2*^{-/-}*Il2rg*^{-/-} mice (Supporting Information Fig. 1D) was similar to blocks in the expression of CD40 and MHCII also reported in CD3 ϵ Tg26 mice 7. Although the signals remain unidentified, our results indicate that lymphoepithelial interactions with DN1–DN3 thymocytes provide differentiation cues that control late stages in the cTEC differentiation program.

Intermediate CCRL1 levels define distinct mTEC subtypes in the postnatal thymus

We reciprocally examined the generation of mTECs relatively to the differentiation of CCRL1-expressing TECs. The primordial CD80⁺ mTECs were found within CCRL1⁺ cells (CCRL1⁺CD80⁺) at E15.5 (Fig. 2A), preceding the complete differentiation of CCRL1^{hi} cTECs around E18.5-postnatal (Fig. 1A). The proportion and number of CCRL1⁺CD80⁺ mTECs augmented throughout time (Fig. 2A and D). Notably, a subset of CD80⁺ TECs, expressing intermediate levels of CCRL1 (CCRL1^{int}CD80⁺), emerged distinctly after birth (Fig. 2A; nonreporter CD80⁺mTECs and *Ccr1* expression are shown in Supporting Information Fig. 2A and B, respectively). As this subtype was virtually absent at E15.5, we compared CCRL1^{int}TECs for the expression of additional cTEC (Ly51) and mTEC (UEA binding) markers 15, 17 in E18.5 and neonatal thymus. At both periods, CCRL1^{hi} and CCRL1⁺CD80⁺ TECs majorly identified either Ly51⁺ cTECs or *Ulex Europaeus* Agglutinin 1 (UEA⁺) mTECs, respectively (Fig. 2A and B). The CCRL1⁺CD80⁺ TECs, which represent a minor subset in the neonatal thymus, were predominantly composed of Ly51^{int}UEA⁺ TECs at this stage. CCRL1^{int} TECs at E18.5 comprised mostly Ly51⁺UEA⁺CD80⁺, although few UEA⁺CD80⁺ and scarce UEA⁺CD80⁺ were detected (Fig. 2B and C). Interestingly, three discrete sizeable subpopulations accumulated within neonatal CCRL1^{int} TECs, including UEA⁺CD80⁺, UEA⁺CD80⁺, and UEA⁺CD80⁺ (Fig. 2C). Both CD80⁺ and CD80⁺ CCRL1^{int}UEA⁺ mTEC subsets, while scarce at E18.5 (Fig. 2B and C), totally represented approximately half and one quarter of the mTEC compartment in neonatal and young thymi, respectively (Fig. 2D). To examine whether CD80⁺CCRL1^{int} mTECs differentiate by the reiteration of the same pathways defined for postnatal mTECs 2, 21, we set E18.5 fetal thymic organ cultures (FTOCs). While rare in intact FTOCs, RANK, and/or CD40 stimulation induced the differentiation of CD80⁺CCRL1^{int} mTECs (Fig. 2E and Supporting Information Fig. 2C and D). Additionally, reaggregate thymic organ cultures (RTOCs) established with E15.5 CCRL1⁺UEA⁺CD80⁺ TECs, and RANK⁺ and CD40-activated to induce mTEC differentiation, showed that a fraction of fetal CCRL1⁺ cTECs displayed CD80⁺ mTEC progenitor activity (Fig. 2F). Next, we analyzed how the phenotypic traits of the emergent neonatal CCRL1^{int} TECs related to the expression of genes linked to cTECs (*Psm11* and *Cst1*) and mTECs (*Tnfrsf11a* (RANK), *Ccl21*, and *Aire*) 2, 3. Increasing *Psm11* and *Cst1* expression was exclusively detected within CCRL1^{int}UEA⁺ and CCRL1^{hi} cells. Interestingly, a gradual increase in *Tnfrsf11a* expression was observed in CCRL1^{int}UEA⁺, CCRL1^{int}UEA⁺CD80⁺, CCRL1^{int}UEA⁺CD80⁺, and CCRL1⁺CD80⁺ TECs. *Ccl21*, which is expressed by postnatal immature mTECs 22, was specifically found within the CCRL1^{int}UEA⁺CD80⁺ and CCRL1^{int}UEA⁺CD80⁺ subsets. Lastly, *Aire* expression was equally enriched in CCRL1⁺ and CCRL1^{int}CD80⁺ mTECs (Fig. 2G). Although fetal CCRL1⁺UEA⁺ TECs have the potential to generate mTECs (Fig. 2F), and the gradual increase in the expression of RANK and CCL21 within CCRL1^{int} cells might suggest a continual stepwise differentiation: CCRL1^{int}UEA⁺ – CCRL1^{int}UEA⁺ – CCRL1^{int}UEA⁺CD80⁺, our attempts to evaluate a direct lineage relationship between neonatal CCRL1^{int} TEC subsets have been unsuccessful, given the difficulty of establishing RTOC with perinatal TECs 23. Thus, we can only speculate that the postnatal cTEC niche harbors progenitors that are able to differentiate into mTECs, as shown in the fetal thymus 15-17. Alternatively, one cannot exclude that postnatal CCRL1^{int} mTECs might differentiate from a lineage unrelated to cTECs. Collectively, our data indicate that while CCRL1^{int}UEA⁺ TECs coexpress molecular traits of cTECs and mTECs, CCRL1^{int}UEA⁺CD80⁺ and CCRL1^{int}UEA⁺CD80⁺ cells define novel subtypes of immature and mature mTECs, respectively, that emerge postnatally.

Thymic selection promotes the generation of CCRL1^{int}mTECs

The differentiation of the CCRL1^{int}CD80⁺ mTECs correlates timely with the intensification of positive thymic selection around the perinatal period 6. Given that activation of RANK and CD40 fostered CCRL1^{int}CD80⁺ mTECs (Fig. 2C) and the ligands for those mTEC-inductive signals are expressed by SP4 thymocytes 2, we investigated whether the appearance of CCRL1^{int}CD80⁺ mTECs depends on TEC-SP4 interactions during selection. To this end we crossed CCRL1-reporter mice onto a Marilyn-*Rag2*^{-/-} TCR transgenic background, in which T cells express an I-A^b-restricted TCR that recognizes the male H-Y antigen 15. As control, we coanalyzed *Rag2*^{-/-} littermates, wherein mTEC differentiation is compromised due to the lack of mature thymocytes 15. Few CD80⁺ mTECs were present in the neonatal *Rag2*^{-/-} thymus, and those were majorly CCRL1⁺ (Fig. 3A-C), resembling mTECs found in the E18.5 thymus (Fig. 2). Contrarily to the normal postnatal thymus, the scarce CCRL1⁺ and CCRL1^{int}CD80⁺ subsets found in *Rag2*^{-/-} mice were predominantly composed of Ly51⁺UEA⁺ cells (Fig. 3A and B). Strikingly, we detected a marked expansion of both CCRL1⁺CD80⁺ and CCRL1^{int}CD80⁺ mTECs in neonatal Marilyn-*Rag2*^{-/-} females (Fig. 3A-C,

nonreporter *Rag2*^{-/-} and Marilyn-*Rag2*^{-/-} are shown in S2E), recapitulating the mTEC composition of the young thymus (Fig. 2A). Akin to the WT thymus, CCRL1^{hi} and CCRL1⁻CD80⁺ TECs specifically identified cTECs and mTECs, respectively, and the emergent CCRL1^{int}CD80⁺ TECs were Ly51^{lo}UEA⁺ (Fig. 3B). One can envision that temporally restricted mTEC differentiation pathways are engaged by interactions between mTEC precursors and distinct hematopoietic cells. As shown previously 10, 11, the generation of the first embryonic mature CD80⁺ mTECs (CCRL1⁻) precedes the development of SP4s and depends on LTβR- and RANK-mediated signaling engaged upon lymphoepithelial interaction with lymphoid tissue inducer cells and γδ T cells 12-14. Our findings indicate that the differentiation of the postnatal-restricted CCRL1^{int}CD80⁺ mTECs results from MHC-TCR, CD40-CD40L, and RANK-RANKL interactions 2, 21 between TEC precursors and TCRβ-selected thymocytes.

CONCLUDING REMARKS

The neonatal life marks a period characterized by a drop in cTECs and an expansion in mTECs 20. The identification of novel postnatal mTEC subsets supports the concept that the foundation of the adult medullary microenvironment results from alternative waves of mTEC differentiation. In this regard, recent evidence suggests that the expansion of the medulla after birth involves de novo formation of mTECs 24. This notion implicates that fetal mTEC precursors might have limited self-renewal potential, as shown for bipotent TEC progenitors 25, and in turn the formation of the adult mTEC niche relies on additional inputs arising after birth. Still, further studies are needed to elucidate to what extent bipotent progenitors might progress through the cortical differentiation program in the adult thymus. Also, the functional relevance of the mTEC heterogeneity reported herein should be further dissected. As mTECs have a crucial role in T-cell maturation and tolerance induction, our findings have implications in therapeutics aimed at modulating TEC niches in the adult thymus.

MATERIALS AND METHODS

Mice

Dual IL-7^{YFP}CCRL1^{GFP} reporter mice were backcrossed onto *Rag2*^{-/-}, *Rag2*^{-/-}*Il2rg*^{-/-}, and Marilyn-*Rag2*^{-/-} C57BL/6 background 8, 15. E0.5 was the day of vaginal plug detection. Animal experiments were performed in accordance with European guidelines.

TEC isolation and flow cytometry

TECs were isolated as described 15. Cells were stained with anti- I-A/I-E (Alexa 780); anti-CD45.2 (PerCP-Cy5.5); anti-EpCAM (A647); anti-CD80 (A660); anti-Ly51, anti-CD205, UEA-1 (biotin), anti-EpCAM (eFluor 450) Abs, and streptavidin (PE-Cy7) (eBioscience). Flow cytometry was performed on a FACSCanto II, with data analyzed on FlowJo software (BD). Cell sorting was performed using the FACSaria I (BD Biosciences), with purities >95%. A 510/10-nm band pass (502LP dichroic mirror) and a 542/27-nm band pass (525LP dichroic mirror) filters were used to discriminate the GFP/YFP signals.

Gene expression

mRNA (RNAeasy MicroKit, Qiagen) isolation and cDNA synthesis (Superscript First-Strand Synthesis System, Invitrogen) were performed as described 15. Real-time PCR (iCycler iQ5) was performed using either TaqMan Universal PCR Master Mix and primers for *18s*, *Ctst*, *Aire*, *Ccl21*, *Tnfrsf11a*, and *Psm11* (Applied Biosystems); or iQ SYBR Green Supermix (Bio-Rad) and primers for *Actb* and *Ccr11* as detailed 15; Triplicated samples were analyzed and the ΔΔCt method was used to calculate relative levels of targets compared with *18s/Actb* as described 15.

FTOCs and RTOCs

FTOCs and RTOCs were established with E18.5 and E15.5 embryos, respectively, as described 15. For FTOCs, TECs were analyzed after 4 days culturing with 1 μg/mL anti-RANK and/or with 5 μg/mL recombinant CD40L (R&D Systems). For RTOCs, 10⁵ E15.5 CCRL1⁺UEA⁻CD80⁻ TECs were sorted and mixed with CD4⁺CD8⁺ and CD4⁺ thymocytes at 1:1:1 ratio. After 3 days, 0.3 μg/mL anti-RANK and 1.3 μg/mL recombinant CD40L were added to the cultures. RTOC were analyzed after 7 days.

Statistical analysis

The unpaired *t* test was used to perform statistical analysis. *p* < 0.05 was considered significant.

Conflict of interest: The authors have no financial or commercial conflicts of interest.

ACKNOWLEDGMENTS

We thank James Di Santo, Jocelyne Demengeot, and Thomas Boehm for *Rag2^{-/-}Il2rg^{-/-}*, CCRL1-reporter, and Marilyn-*Rag2^{-/-}* mice, respectively. We thank Dr. Catarina Leitão for critical reading of the manuscript and technical assistance. We thank FEDER funds through the Operational Competitiveness Programme – COMPETE and by National Funds through *Fundação para a Ciência e a Tecnologia*(FCT) under the project PTDC/SAU-IMU/117057/2010 funded this work. N.L.A., A.R.R., C.M., and P.M.R. are supported by FCT Investigator program and PhD fellowships.

ABBREVIATIONS

Aire - auto-immune regulator
CCRL1- chemokine (C-C motif) receptor-like 1
cTEC - cortical TEC
FC - flow cytometry
FTOC - fetal thymic organ culture
LTβR - lymphotoxin beta receptor
mTEC - medullary TEC
RANK - receptor activator of NF-κB
ROTC - reaggregate thymic organ culture
SP - single positive
TEC - thymic epithelial cell
UEA - *Ulex Europaeus* Agglutinin 1

REFERENCES AND NOTES

1. Takahama, Y., Journey through the thymus: stromal guides for T-cell development and selection. *Nat. Rev. Immunol.* 2006. 6: 127–135.
2. Anderson, G. and Takahama, Y., Thymic epithelial cells: working class heroes for T cell development and repertoire selection. *Trends Immunol.* 2012. 33: 256–263.
3. Mathis, D. and Benoist, C., Aire. *Annu. Rev. Immunol.* 2009. 27: 287–312.
4. Rossi, S. W., Jenkinson, W. E., Anderson, G. and Jenkinson, E. J., Clonal analysis reveals a common progenitor for thymic cortical and medullary epithelium. *Nature* 2006. 441: 988–991.
5. Bleul, C. C., Corbeaux, T., Reuter, A., Fisch, P., Monting, J. S. and Boehm, T., Formation of a functional thymus initiated by a postnatal epithelial progenitor cell. *Nature* 2006. 441: 992–996.
6. Anderson, G., Jenkinson, E. J. and Rodewald, H. R., A roadmap for thymic epithelial cell development. *Eur. J. Immunol.* 2009. 39: 1694–1699.
7. Shakib, S., Desanti, G. E., Jenkinson, W. E., Parnell, S. M., Jenkinson, E. J. and Anderson, G., Checkpoints in the development of thymic cortical epithelial cells. *J. Immunol.* 2009. 182: 130–137.
8. Alves, N. L., Huntington, N. D., Mention, J. J., Richard-Le Goff, O. and Di Santo, J. P., Cutting edge: a thymocyte-thymic epithelial cell cross-talk dynamically regulates intrathymic IL-7 expression in vivo. *J. Immunol.* 2010. 184: 5949–5953.
9. Ripen, A. M., Nitta, T., Murata, S., Tanaka, K. and Takahama, Y., Ontogeny of thymic cortical epithelial cells expressing the thymoproteasome subunit beta5t. *Eur. J. Immunol.* 2011. 41: 1278–1287.
10. Hamazaki, Y., Fujita, H., Kobayashi, T., Choi, Y., Scott, H. S., Matsumoto, M. and Minato, N., Medullary thymic epithelial cells expressing Aire represent a unique lineage derived from cells expressing claudin. *Nat. Immunol.* 2007. 8: 304–311.

- 11.White, A. J., Withers, D. R., Parnell, S. M., Scott, H. S., Finke, D., Lane, P. J., Jenkinson, E. J. et al., Sequential phases in the development of Aire-expressing medullary thymic epithelial cells involve distinct cellular input. *Eur. J. Immunol.* 2008. 38: 942–947.
- 12.Rossi, S. W., Kim, M. Y., Leibbrandt, A., Parnell, S. M., Jenkinson, W. E., Glanville, S. H., McConnell, F. M. et al., RANK signals from CD4(+)3(-) inducer cells regulate development of Aire-expressing epithelial cells in the thymic medulla. *J. Exp. Med.* 2007. 204: 1267–1272.
- 13.Roberts, N. A., White, A. J., Jenkinson, W. E., Turchinovich, G., Nakamura, K., Withers, D. R., McConnell, F. M. et al., Rank signaling links the development of invariant gammadelta T cell progenitors and Aire(+) medullary epithelium. *Immunity* 2012. 36: 427–437.
- 14.Mouri, Y., Yano, M., Shinzawa, M., Shimo, Y., Hirota, F., Nishikawa, Y., Nii, T. et al., Lymphotoxin signal promotes thymic organogenesis by eliciting RANK expression in the embryonic thymic stroma. *J. Immunol.* 2011. 186: 5047–5057.
- 15.Ribeiro, A. R., Rodrigues, P. M., Meireles, C., Di Santo, J. P. and Alves, N. L., Thymocyte selection regulates the homeostasis of IL-7-expressing thymic cortical epithelial cells in vivo. *J. Immunol.* 2013. 191: 1200–1209.
- 16.Baik, S., Jenkinson, E. J., Lane, P. J., Anderson, G. and Jenkinson, W. E., Generation of both cortical and Aire(+) medullary thymic epithelial compartments from CD205(+) progenitors. *Eur. J. Immunol.* 2013. 43: 589–594.
- 17.Ohigashi, I., Zuklys, S., Sakata, M., Mayer, C. E., Zhanybekova, S., Murata, S., Tanaka, S. et al., Aire-expressing thymic medullary epithelial cells originate from beta5t-expressing progenitor cells. *Proc. Natl. Acad. Sci. USA* 2013. 110: 9885–9890.
- 18.Alves, N. L., Takahama, Y., Ohigashi, I., Ribeiro, A. R., Baik, S., Anderson, G. and Jenkinson, W. E., Serial progression of cortical and medullary thymic epithelial microenvironments. *Eur. J. Immunol.* 2014. 44: 16–22.
- 19.Rodewald, H. R., Paul, S., Haller, C., Bluethmann, H. and Blum, C., Thymus medulla consisting of epithelial islets each derived from a single progenitor. *Nature* 2001. 414: 763–768.
- 20.Rode, I. and Boehm, T., Regenerative capacity of adult cortical thymic epithelial cells. *Proc. Natl. Acad. Sci. USA* 2012. 109: 3463–3468.
- 21.Akiyama, T., Shimo, Y., Yanai, H., Qin, J., Ohshima, D., Maruyama, Y., Asaumi, Y. et al., The tumor necrosis factor family receptors RANK and CD40 cooperatively establish the thymic medullary microenvironment and self-tolerance. *Immunity* 2008. 29: 423–437.
- 22.Lkhagvasuren, E., Sakata, M., Ohigashi, I. and Takahama, Y., Lymphotoxin beta receptor regulates the development of CCL21-expressing subset of postnatal medullary thymic epithelial cells. *J. Immunol.* 2013. 190: 5110–5117.
- 23.Rossi, S. W., Chidgey, A. P., Parnell, S. M., Jenkinson, W. E., Scott, H. S., Boyd, R. L., Jenkinson, E. J. et al., Redefining epithelial progenitor potential in the developing thymus. *Eur. J. Immunol.* 2007. 37: 2411–2418.
- 24.Dumont-Lagace, M., Brochu, S., St-Pierre, C. and Perreault, C., Adult thymic epithelium contains non-senescent label-retaining cells. *J. Immunol.* 2014. 192: 2219–2226.
- 25.Jenkinson, W. E., Bacon, A., White, A. J., Anderson, G. and Jenkinson, E. J., An epithelial progenitor pool regulates thymus growth. *J. Immunol.* 2008. 181: 6101–6108.

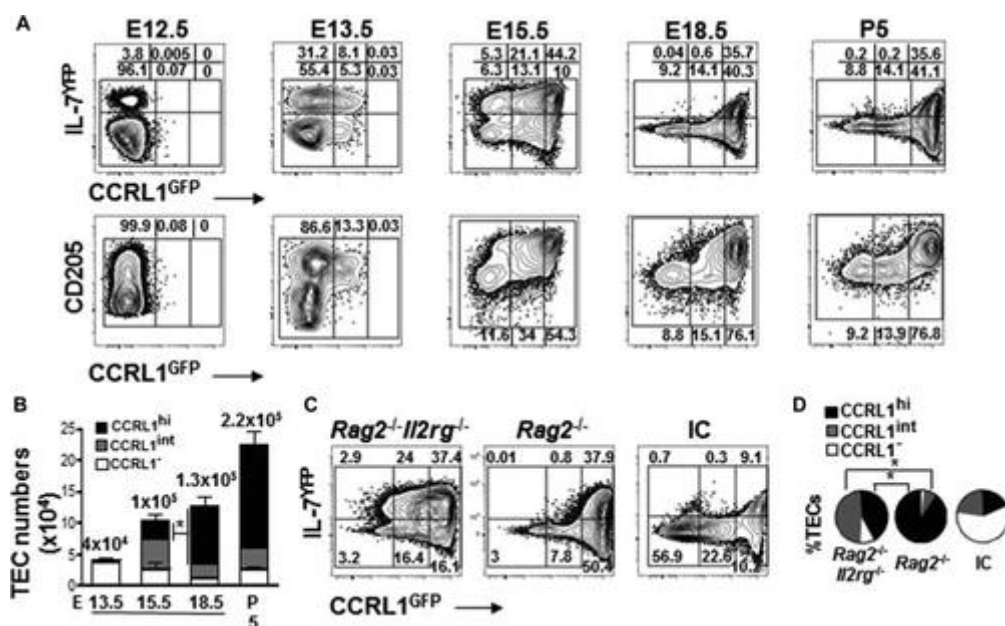


Figure 1

CCRL1 is a late cTEC determinant. (A) Total TECs (gated as CD45-EpCAM⁺) from IL-7^{YFP}CCRL1^{GFP} mice were analyzed for IL-7^{YFP} and CCRL1^{GFP} or CD205 and CCRL1^{GFP} expression by flow cytometry (FC) at the indicated time points. Numbers in plots indicate the frequency of cells found within each gate. Plots are representative of three to five independent experiments per time point. E represents embryonic day and P5 represents postnatal day 5. (B) Cellularity of TECs expressing high (CCRL1^{hi}), intermediate (CCRL1^{int}), and no CCRL1 (CCRL1⁻) was determined by the absolute thymic cell numbers and the respective frequencies of each subset obtained by FC. Numbers on top of bars indicate average TEC cellularity for each time point. Data are shown as mean + SD of 3–5 samples pooled from three to five independent experiments. **p* < 0.05 (unpaired *t* test). (C) TECs from 2-week-old *Rag2*^{-/-}, *Rag2*^{-/-}*Il2rg*^{-/-}, and immunocompetent (IC) thymi were analyzed by FC for IL-7^{YFP} and CCRL1^{GFP} expression. Numbers in plots indicate the frequency of each gate. Plots are representative of three independent experiments. (D) The mean proportion (%) of CCRL1 subsets in 2-week-old *Rag2*^{-/-}, *Rag2*^{-/-}*Il2rg*^{-/-}, and IC mice, determined by FC, is depicted. **p* < 0.001 (unpaired *t* test). Data represent means of three to five experiments (*n* = 5–6 mice/group).

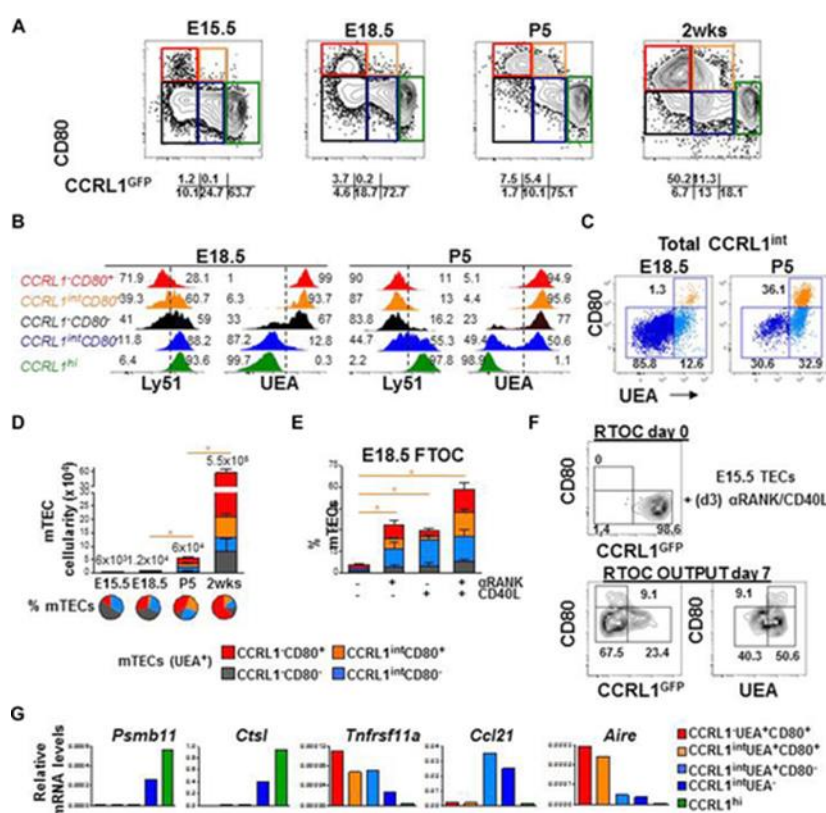


Figure 2

Intermediate CCRL1 expression reveals novel postnatal mTECs. (A) TECs (gated as CD45-EpCAM⁺) from IL-7^{YFP}CCRL1^{GFP} mice were analyzed for CCRL1^{GFP} and CD80 expression by FC at the indicated time points. Colored gates define different subsets and grids indicate the frequencies of each respective one. (B) TEC subsets defined by the colored gates in (A) from E18.5 and postnatal day 5 (P5) thymi were analyzed for Ly51 and UEA expression by FC. Numbers in histograms indicate the frequency within each gate. Histograms are representative of three to five independent experiments. (C) Expression of UEA and CD80 within gated E18.5 and postnatal day 5 (P5) total CCRL1^{int} TECs was determined by FC. Numbers in plots indicate the frequency of cells found within each gate. (A–C) Plots are representative of three to five independent experiments. (D) Cellularity of UEA⁺ mTEC subsets from IL-7^{YFP}CCRL1^{GFP} mice was assessed as in Figure 1. Average total mTEC cellularity is detailed above bars. Pie graphs represent the mean proportion of color-coded subsets within total UEA⁺ mTECs. **p* < 0.05 (unpaired *t* test) (data are shown as mean + SD of 4–6 mice/group, pooled from three to five independent experiments) (E) E18.5 FTOCs were cultured for 4 days with the indicated stimuli and then assessed for mTEC induction (UEA⁺CD80⁺/-) by FC. The proportion of subsets within UEA⁺ mTECs is color-coded. Data are shown as mean + SD of 8–10 thymic lobes/group, pooled from three independent experiments. **p* < 0.05 (unpaired *t* test). (F) RTOCs established with E15.5-derived CCRL1⁺UEA⁻CD80⁻ TECs were stimulated with αRANK and/or CD40L and gated TECs were analyzed for the expression of the indicated markers by FC. Plots are representative of three independent experiments. (G) Expression of *Psm11*, *Cts1*, *Tnfrsf11a*, *Ccl21*, and *Aire* was assessed by qPCR in purified TEC subsets (colored columns) from postnatal day 5 (P5) IL-7^{YFP}CCRL1^{GFP} mice. Values were normalized to 18s. Data are shown as representative of three independent experiments.

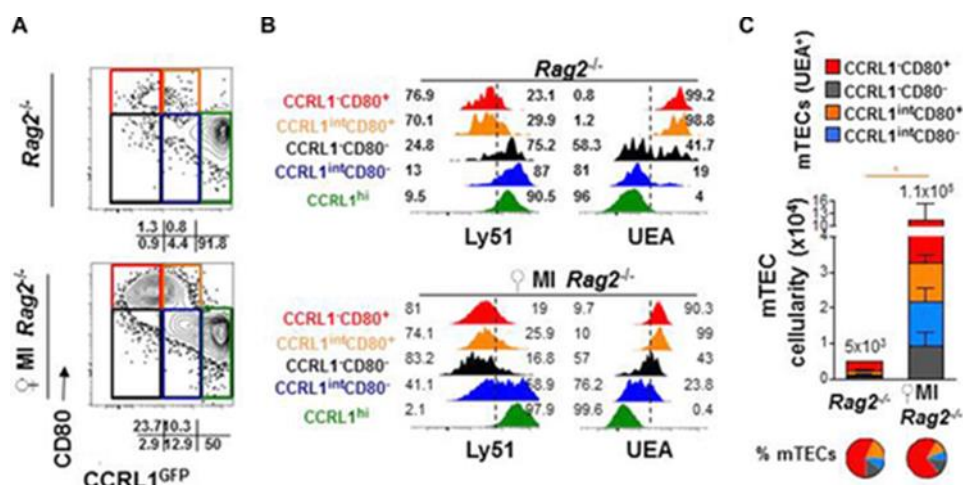


Figure 3

Thymic selection drives the emergence of the postnatal-specific CCRL1^{int}CD80⁺TECs. (A) TECs (gated as CD45-EpCAM⁺) from postnatal day 5 (P5) *Rag2*^{-/-} and female Marilyn-*Rag2*^{-/-} mice were analyzed for CCRL1^{GFP} and CD80 expression by FC. Colored boxes define different TEC subsets and grids indicate the frequencies of each one. Plots are representative of two to three independent experiments. (B) Subsets defined by the colored gates in (A) from *Rag2*^{-/-} and Marilyn-*Rag2*^{-/-} mice were analyzed for Ly51 and UEA expression by FC. Numbers in histograms indicate the frequency within each gate. Histograms are representative of three independent experiments. (C) Frequency of subsets within total mTECs (pie graphs) and numbers of mTEC subsets was determined by FC. Data are shown as mean + SD of three to five samples, pooled from two independent experiments. **p* < 0.05 (unpaired *t* test).